Efficiency of pyoverdines in iron removal from flocking asbestos waste: An innovative bacterial bioremediation strategy

Sébastien R David, Dris Ihiawakrim, Robert Regis, Valérie Geoffroy

Efficiency of pyoverdines in iron removal from flocking asbestos waste: an innovative bacterial bioremediation strategy

Sébastien R. David[a,b], *Dris Ihiawakrim*[c], *Robert Regis*[d], *Valérie A. Geoffroy*[a]*

[a] Université de Strasbourg, CNRS-UMR7242, BSC, ESBS, 300 Bld Sébastien Brant, 67413 Illkirch, Strasbourg, France

[b] Agence de l'Environnement et de la Maîtrise de l'Energie, 20 avenue du Grésillé, BP 90406, 49004 Angers Cedex 01, France

[c] Université de Strasbourg, CNRS-UMR7504, IPCM, 23 rue du Loess, BP 43, 67034 Strasbourg, France

[d] SOMEZ, Parc Marcel Dassault, 470 Rue Alberto Santos Dumont, 34430 Saint Jean de Vedas, France

*** Corresponding authors :** V. A. Geoffroy, UMR 7242, Université de Strasbourg-CNRS, ESBS, Biotechnologie et Signalisation Cellulaire, Bd Brant, CS 10413, F-67412 Illkirch Cedex France.

Email : valerie.geoffroy@unistra.fr

Tel. (+33) 3 68 85 47 51

Fax (+33) 3 68 85 48 29

Abstract

The use of asbestos-containing products has been banned in many countries since the beginning of the 80's due to its carcinogenic properties. However, asbestos is widely present in private and public buildings, resulting in the need to process a vast amount of asbestos-containing waste. Among the current technologies for the destruction of asbestos fibers, biodegradation by fungi, lichens, and, more recently, bacteria has been described. We previously reported the involvement of the bacterial siderophore pyoverdine in the release of iron from the two asbestos groups, serpentines and amphiboles. Among the large diversity encountered in the pyoverdine family, we examined whether these siderophores can alter flocking asbestos waste as well. All the tested pyoverdines were efficient in chrysotile-gypsum and amosite-gypsum weathering, although some exhibited higher iron dissolution. Iron was solubilized by pyoverdines from *Pseudomonas aeruginosa* and *mandelii* in a time-dependent manner from chrysotile-gypsum within 24 hours. Renewal of pyoverdine-containing supernatant every 24 or 96 hours allowed iron removal from chrysotile-gypsum at each cycle, until a limit was reached after 42 days of total incubation. Moreover, the dissolution was concentration-dependent, as demonstrated for the pyoverdine of

P. *mandelii*. Pyoverdine-asbestos weathering could therefore become an innovative method to reduce anthropogenic waste.

Keywords
Pyoverdine- *Pseudomonas*-Asbestos-Iron-Alteration

1. Introduction

Asbestos has been extensively used because of its excellent properties, such as thermal conductivity, high mechanical strength, resistance to chemical attacks, and low cost. Asbestos is composed a group of fibrous silicate minerals that belong to the serpentine and amphibole families. Amphiboles can contain up to 36% iron by weight, whereas the serpentine form of asbestos contains only 2 to 3% iron by weight (Chao and Aust, 1994). Iron can be present as part of the mineral structure in the amphibole or as an exchangeable element in the chrysotile (Douguet et al., 1997; Virta, 2002). The iron encountered in asbestos is able to catalyze many reactions, such as lipid peroxidation, oxygen consumption, ROS formation, and DNA damage, precursors for tumor development (Toyokuni, 2009; Valko et al., 2015). The various types of toxic effects in humans include fibrogenesis and stomach, ovarian, and lung cancer (Scherpereel, 2016). Due to the associated health problems, asbestos was banned after more than 30 years of intense use. As a consequence, we are confronted with the generation of a vast amount of asbestos-containing waste (ACW).

Today, most waste is packed and deposited in controlled landfills, an inexpensive technique that does not remove the toxicity or potential health risk of waste related to fiber inhalation (Spasiano and Pirozzi, 2017). ACW treated by stabilization aims to reduce the fibers released, without modifying the crystalline structure, and ends up in landfills. The second type of treatment, called inertization, consisting of thermal treatment (vitrification or microwave), or hydrothermal, chemical, or mechanochemical treatment, involves the total transformation of the fibers, providing an inert and harmless material, considered to be a resource. However, such thermal treatment is expensive due to energy consumption and may release emissions into the atmosphere. Chemical treatment requires chemical products and their disposal, but has allowed confirmation of the potential Mg released (Paolini et al., 2019). At the laboratory scale, bioremediation experiments have been carried out on raw asbestos using various organisms

(fungi, lichens, or bacteria) or metabolites (organic acids or siderophores), whereas few studies have focused on ACW. A few studies have focused on asbestos-cement waste, whereas none have investigated biological treatment of flocking asbestos waste (FAW), of which the matrix composition differs, containing gypsum to allow flocking to walls instead of cement. For example, lichens are able to cover asbestos-cement roofs and modify the surface reactivity, leading to bioavailable iron and magnesium liberation (Favero-Longo et al., 2009). Moreover, modification of the fibers has been described, by which they became amorphous, due to oxalic acid production (Favero-Longo et al., 2005) and nitrous and nitric acid produced by nitrifying bacteria, such as *Nitrosomonas* and *Nitrobacter*, inducing corrosion of a cement-roof, thus increasing porosity and reducing the strength of the material (Wasserbauer et al., 1988). Moreover, Wang et al. (2010, 2011) also highlighted the porous structure of cement pipes after microorganism colonization. They showed that acid-producing bacteria together with slime-forming and heterotrophic bacteria contribute to corrosion of the inside surface of asbestos-cement pipes of water distribution systems. Innovative bio-chemical processes have been recently proposed, in which the cement phase is dissolved by lactic acid produced by *Lactobacilli* or by dark fermentation, before hydrothermal end treatment (Balducci et al., 2012; Spasiano et al., 2017). Siderophore production is a common mechanism shown in fungal and bacterial weathering of native asbestos, leading to iron dissolution from fibers (Daghino et al., 2010; Rajkumar et al., 2009). Siderophores are a well-known strategy that many living organisms use to access iron, an essential element for growth. In mineral-bacterial weathering, various siderophores have been implicated in iron dissolution, resulting in leaching of the material, and pyoverdine (PVD) has been described to interact with iron-bearing silicates, such as smectite (Ferret et al., 2014) and municipal waste-bottom ashe (Aouad et al., 2008). However, this mechanism has not yet been investigated on ACW. We thus investigated the impact of the bacterial siderophore PVD, produced by fluorescent *Pseudomonas*, on FAW. In building construction, two types of FAW have been described, varying in texture, thickness, and density. The first type used in this study contained 50 to 90% chrysotile fibers ($(Mg_3Si_2O_5(OH)_4$) and 10 to 50% gypsum ($CaSO_4$, $2H_2O$), whereas the second contained 5 to 30% chrysotile fibers and 95 to 70% gypsum. Amphibole fibers, such as amosite ($(Fe, Mg)_7Si_8O_{22}(OH)_2$), have also sometimes been combined with FAW. The ability of pyoverdine to extract iron from fiber has

already shown on chrysotile and amphibole raw asbestos. However, two main difficulties such as the iron pollution present in the matrix and the fiber accessibility may interfere with the iron extraction by pyoverdine.

Among the 100 PVDs so far described by siderotyping fluorescent *Pseudomonas*, their affinity for iron is not yet known. We therefore tested several representatives from the PVD laboratory collection to determine their ability to scavenge iron from ACW and selected the most efficient. Iron removal was tested as a function of PVD concentration and the optimum time for FAW alteration determined. Long-term alteration experiments by the best identified PVDs determined the iron extraction limit.

2. Experimental

2.1 Asbestos wastes preparation

Two types of flocking asbestos wastes were used, chrysotile-gypsum and amosite-gypsum. These wastes come from the asbestos removal site of Jussieu University of Paris and kindly provided by the Mediterranean Company of Zeolites (SOMEZ). To obtain amosite-gypsum, FAW samples were incubated in an acidic bath with sulfuric acid (8 mol/L), until total dissolution of the chrysotile brucite layer. All asbestos samples (0.2 g) were sterilized by autoclave (121°C for 20 min) and incubated at 70°C for 14 days before experiments. Before each experiment, asbestos samples were washed with 20 mL of sterile succinate medium to remove free Fe and Mg.

2.2 Bacterial strains

Bacteria used in this study were listed in table 1. Strains were stored in LB-20 % glycerol stock at -80°C. *Pseudomonas* cells were grown routinely overnight at 30°C in Luria Bertani medium (LB) under shaking condition (220 rpm).

2.3 Production of pyoverdines

1 mL of overnight LB culture of *Pseudomonas* strains was centrifuged (3 min at 9871 g). For iron starved cells, the iron-deficient succinate medium (composition in $g.L^{-1}$: K_2HPO_4, 6.0;

120 KH_2PO_4, 3.0; $(NH_4)_2SO_4$, 1.0; $MgSO_4.7H_2O$, 0.2; sodium succinate, 4.0; pH adjusted to 7.0 by
121 addition of NaOH), sterilized by 0.2 µm filtration, was used (Meyer and Abdallah, 1978). The
122 pellet, washed twice with 1 ml of sterile succinate medium, was suspended in 1 ml of sterile
123 succinate medium and inoculated in 15 mL of sterile succinate medium, incubated at 30°C under
124 shaking condition (220 rpm). After 24 h of growth, 7.5 mL of this culture was transferred in an
125 Erlenmeyer flask containing 1 L of sterile succinate medium. After 24 h of incubation at 30°C
126 under shaking condition (220 rpm), the culture was centrifuged (2664 g for 40 min). The
127 supernatant was filtered twice with glass microfibre filters (Whatman, GF/C) and once on
128 nitrocellulose filter (0.45 µm porosity). To determine pyoverdine concentration, OD_{400} was
129 measured with a Specord 205 spectrophotometer (Analytik Jena). When needed, the PVD
130 concentration was adjusted with purified PVD according to the method described so far.
131 Siderophore containing supernatant was loaded, after acidification (pH 6.0), on XAD-4 column,
132 washed with two volume of purified water and eluted with one volume of 50% ethanol. The
133 eluate was concentrated under vacuum on a rotary evaporator and lyophilized.
134
135 **2.4 Asbestos dissolution by pyoverdines**

136 To evaluate the effect of various PVDs on the dissolution of iron from chrysotile-gypsum
137 and amosite-gypsum, 20 mL of PVD-containing supernatants adjusted to 100 µM were incubated
138 with materials in 50 mL Falcon tubes. After 24 h of incubation at 30°C under shaking condition
139 (220 rpm), the assays were centrifuged 30 min at 9871 g to recover supernatants. Assays were
140 done in 3 to 5 replicates.
141 Kinetics of iron dissolution from chrysotile-gypsum in 20 mL of PVD-containing
142 supernatant of *P. aeruginosa* and *P. mandelii* respectively adjusted to 100 µM were followed on
143 24 hours with regular sampling of the solution at 1, 2, 4, 6, 8 and 24 h. Assays were done in 5
144 replicates.
145 Long-term alteration of chrysotile-gypsum by PVD-containing supernatant of *P.*
146 *aeruginosa* and *P. mandelii* was performed by renewal cycles at 30°C under shaking condition
147 (220 rpm). Nine cycles of 24 hours and seven cycles of 96 h were realized in the presence of 100
148 µM of PVD-containing supernatant, followed by a 24 and a 96 h cycles with 200 µM of PVD-
149 containing supernatant. Assays were done in 5 replicates.

To determine the effect of pyoverdine concentrations produced by *P. mandelii* on iron and magnesium dissolution from chrysotile-gypsum, material was incubated during 48 h at 30°C under shaking condition (220 rpm) with 20 mL of supernatant adjusted to 25, 50, 100, 150 and 200 µM. Assays were done in 5 replicates.

Materials were eliminated from supernatants by filtration (0.22 µm porosity). Iron and magnesium content were measured depending on the experiment.

2.5 Determination of Fe and Mg contents

In order to determine iron content, we used the bathophenanthroline method, which is a sensitive colorimetric method for determining ferrous iron content. To determine the total iron, ferric iron was converted to ferrous iron by thioglycolic acid. Each sample was analyzed in triplicate. 20 µL of sample were dispensed into each well of a 96-well plate (Greiner, PS flat-bottomed microplate). 40 µL of saturated sodium acetate (5.5 M) (Sigma-Aldrich), 80 µL of cold distilled water, 10 µL of a thioglycolic acid solution diluted 10 times in water (Sigma-Aldrich) and 10 µL of bathophenanthroline (5 $mg.mL^{-1}$) (Sigma-Aldrich) were additionned per well. After shaking, microplates were stored overnight at 4°C. Absorbance was measured at 535 nm in a Tecan microplate reader (Infinite M200, Tecan) and iron concentration ($mg.L^{-1}$) was determined by reference to a standard curve.

For the magnesium content, calmagite method was used. Magnesium formed a coloured complex with calmagite. EGTA (Ethylene Glycol Tetraacetic Acid) was used to eliminate any calcium interference. Each sample was analyzed in triplicate. To prepare the reactive solution, one volume of reagent 1 (1 $mol.L^{-1}$ of 2-Methyl-2-Amino-1-Propanol and 215 $\mu mol.L^{-1}$ of EGTA) with one volume of reagent 2 (300 $\mu mol.L^{-1}$ of calmagite) were mixed. 3 µL of sample were dispensed into each well of a 96-well plate (Greiner, PS flat-bottomed microplate) and 300 µL of reactive solution mixed were added. After shaking and 30 seconds of incubation, absorbance was measured at 500 nm in a Tecan microplate reader (Infinite M200, Tecan) and magnesium concentration ($mg.L^{-1}$) was determined by reference to a standard curve.

2.6 STEM-EDX of asbestos fibers

TEM (Transmission Electron Microscopy) images were recorded with a JEOL 2100 microscope, with a 200 kV potential applied on a LaB6 filament as an electron source. Resolution of the TEM is 0.21 nm. TEM mapping was performed in STEM (Scanning transmission electron microscopy) mode (resolution 2 nm) and using an SSD-EDX (Silicon Drift Detector-Energy Dispersive X-ray) spectrometer to determine the chemical composition.

2.7 Statistical analysis

Results presented in all figures correspond to mean values of three to five replicates. Significant statistical differences among values were determined using Kruskal-Wallis test (RStudio v1.0.153) followed by a Conover post-hoc analysis. Values with the same letter are not significantly different at $p = 0.05$.

3. Results and discussion

3.1 Efficiency of pyoverdines on iron removal from flocking asbestos wastes

PVDs, yellow-green fluorescent pigments, are composed of three moieties: (i) a peptide chain varying in the nature, number, and order of amino acids, (ii) a dihydroxyquinoline chromophore, conferring the yellow-green color of the molecule, and (iii) an acyl chain radical made of dicarboxylic acid residue which can be either succinate, malate, or their amide forms, or alpha-ketogluratate or glutamate, depending on the producing strain and growth conditions. Based on these structural differences, PVDs have been purified from various *Pseudomonas* strains to obtain a large family composed of more than 100 different structures, depending on their peptide chain and radical R (Meyer et al., 1998). PVD binds to Fe^{3+} in a 1:1 stoichiometry with a stability constant for Fe(III) of approximately 10^{32} M^{-1} for PVD produced by *P. aeruginosa* PAO1 (Albrecht-Gary et al., 1994). From this bank, we selected nine PVDs produced by various *Pseudomonas* species based on their different isoelectrofocusing profile related to the length, nature, and presence of cycle rings in the peptide chain (Table 1). These selected PVDs were tested to investigate potential differences in their ability to chelate iron. We previously showed that purified PVDs can extract iron from the three native asbestos types, chrysotile, amosite, and crocidolite, and with the same efficiency as PVD-containing supernatant (David et

al., 2019). Therefore, we used PVD-containing supernatants to determine the effect of these siderophores on FAW, chrysotile-gypsum, and amosite-gypsum (Fig. 1). The nine selected PVDs (at a concentration of 100 μM) were incubated with each FAW for 24 h. The control medium (sterile succinate medium) had no visible effect on iron dissolution from waste, whereas all tested PVDs exhibited significant iron extraction from both types of waste, ranging from 0.24 $mg.L^{-1}$ to 1.22 $mg.L^{-1}$ iron dissolved for chrysotile-gypsum and 0.63 to 5.39 $mg.L^{-1}$ for amosite-gypsum. For chrysotile-gypsum, 25% of the siderophores were in the PVD-Fe complex form, whereas PVD was almost saturated at 100% for amosite-gypsum, a factor that may have limited material weathering. A higher amount of extracted iron was obtained for amosite-gypsum, which is consistent with the chemical composition of this material, which contains more iron than chrysotile-gypsum. Iron removal was not the same for all PVDs. Moreover, the PVD which extracted the most iron was different, depending on the type of waste: PVD from *P. mandelii* for chrysotile-gypsum, with 1.22 $mg.L^{-1}$, and *P. fluorescens* for amosite-gypsum, with 5.39 $mg.L^{-1}$. In addition, the amount of iron extracted from samples incubated in fresh supernatants for 48 h was the same as that measured after 24 h (data not shown). Studies examining siderophore-mediated iron dissolution from chrysotile waste are lacking. A few studies have focused on the effect of the commercial bacterial siderophore desferrioxamine, produced by *Streptomyces pilosus*, on asbestos fibers. Iron removal from crocidolite and amosite by this siderophore is also effective (Chao and Aust, 1994). Moreover, Mohanty et al. (2018) showed that desferrioxamine releases exchangeable and structural iron from chrysotile fibers in a concentration-dependent manner. Other studies have shown that fungal strains can extract iron from asbestos, likely promoted by siderophores (Daghino et al., 2008). Mohanty et al. (2018) showed that desferrioxamine was as effective as the fungi siderophore, ferrichrome, in removing iron from chrysotile fibers.

3.2 Kinetics of iron extraction from chrysotile-gypsum by pyoverdines

We then focused on the most representative ACW among waste, chrysotile-gypsum. Based on the results show in Fig. 1, we carried out waste alteration using the two PVD-containing supernatants from *P. aeruginosa* ($PVD_{aeruginosa}$) and *P. mandelii* ($PVD_{mandelii}$), adjusted to a final concentration of 100 μM (Fig. 2). We sampled and measured iron solubilization during the

first 8 h and at the end of the incubation to better understand the iron extraction kinetics. The kinetic profiles of dissolution by the two PVDs were very similar and achieved the same iron extraction (0.9 $mg.L^{-1}$) at the end of the experiment, consistent with the results presented in Fig. 1. We detected dissolved iron for $PVD_{mandelii}$ and $PVD_{aeruginosa}$ after only 1 h of contact (0.12 and 0.17 $mg.L^{-1}$, respectively), which progressively increased during the next 8 h of dissolution (0.59 and 0.54 $mg.L^{-1}$, respectively). The same time scale of 24 h was used by Mohanty et al. (2018) to reach an iron dissolution equilibrium for chrysotile fiber weathering by desferrioxamine. However, we cannot compare the iron concentrations because our experiment focused on chrysotile waste embedded in gypsum for flocking purposes in housing, whereas that of Mohanty *et al*. used raw asbestos fibers.

3.3 Long-term alteration of chrysotile-gypsum by pyoverdines

Our experiments clearly show that the optimum time for chrysotile-gypsum alteration is 24 h without renewal of the medium. We conducted a second set of experiments, with periodic medium renewal, for 42 days on FAW to determine the limit of iron extraction by PVDs produced by *P*. *aeruginosa* and *P*. *mandelii*. The supernatant was replaced by fresh apo-PVD supernatant at each cycle. $PVD_{aeruginosa}$ and $PVD_{mandelii}$ showed equivalent iron release over time, which is consistent with the previous results. Succinate medium alone had no effect on iron dissolution, as only low iron concentrations were detected in the control (0.01 to 0.08 $mg.L^{-1}$) (Fig. 3). During the 24 h cycles (T24-1 to T24-8), using siderophore concentrations of 100 µM, iron extraction decreased from 0.92 to 0.28 $mg.L^{-1}$ for $PVD_{aeruginosa}$ and 0.88 to 0.22 $mg.L^{-1}$ for $PVD_{mandelii}$. We observed an unexpected increase to 0.42 for $PVD_{aeruginosa}$ and 0.37 for $PVD_{mandelii}$ for T24-9, due to a longer stand-by period (a week) between T24-8 and T24-9 than for the other cycles, for which the duration was < 72 h. Thus, the cycles were extended to 96 h for seven cycles. At T96-1, iron dissolution was 0.55 $mg.L^{-1}$ for $PVD_{aeruginosa}$ and 0.45 $mg.L^{-1}$ for $PVD_{mandelii}$. After T96-2, released iron decreased to 0.24 $mg.L^{-1}$ for $PVD_{aeruginosa}$ and 0.25 $mg.L^{-1}$ for $PVD_{mandelii}$ and remained constant between T96-5 and T96-7. Then, we incubated

265 the chrysotile-gypsum in a 200 µM PVD-containing supernatant for 24 and 96 h to determine
266 whether additional iron could be extracted. However, the concentration of solubilized iron was
267 very low (0.17 for $PVD_{aeruginosa}$ and 0.09 $mg.L^{-1}$ for $PVD_{mandelii}$ after 96 h*)*. The waste
268 contains chrysotile, with a theoretical composition of $Mg_3Si_2O_5(OH)_4$, which is a sheet silicate
269 composed of inner tetrahedral silicate layers and outer magnesium oxide octahedral layers
270 (brucite). Since asbestos originated from soils where iron is highly abundant, magnesium in the
271 outer layer may be replaced by ferrous and ferric iron. The same phenomenon may occur in the
272 inner silicate layer, where silicon may be exchanged by ferric iron only (Pollastri et al., 2015). In
273 our study, some iron appeared to be more easily solubilized during short-term assay (24 h),
274 whereas we needed to increase the exposure time to 96 h to continue iron dissolution. It is well
275 known that siderophore-mediated iron removal leads to siderophore adsorption on the iron-
276 bearing mineral surface. For example, PVD has already been shown to dissolve structural iron
277 from smectite upon contact (Ferret et al., 2014). A few studies have focused on siderophore
278 dissolution mechanism for mineral asbestos. Mohanty et al. (2018) studied iron release from
279 chrysotile fibers, depending on the concentration of desferrioxamine in long-term experiments
280 with no solution renewal. The low concentration of desferrioxamine (1 µM) released some iron
281 from the surface of the brucite layer, whereas increasing the concentration of desferrioxamine to
282 10 µM led to better surface coverage. Exhaustion of surface sites could provide easier access to
283 the iron present in the silica tetrahedron. In our experiment, the concentration of both
284 siderophores remained predominantly constant (100 µM) and the solutions were renewed at
285 regular intervals of 24 h or 96 h. Our results tend to point to the same conclusion as those of
286 Mohanty et al. (2018), in which short renewal cycles appear to release iron from the brucite
287 layer, leaching the fiber surface and potentially providing access to iron from the silica layer.
288 The increase in iron removal by the 96 h renewal cycles could be explained by two mechanisms:
289 i) better siderophore surface coverage and the ii) release of iron from the silica layer. As iron
290 dissolution from the silica tetrahedron could be slow, our long renewal cycles may have
291 facilitated such weathering.
292 Analysis of chrysotile fibers by STEM-EDX (Fig. 4) showed a large decrease of iron
293 content after long-term alteration with both PVDs and confirms that iron was removed from the

structure. Interestingly, the silica content tended also to decrease after PVD contact. These results confirm active dissolution driven by the siderophores.

3.4 Effect of pyoverdine concentrations on iron and magnesium dissolution from chrysotile-gypsum

Various concentrations of $PVD_{mandelii}$ were added to FAW over 48 h to evaluate iron and magnesium release. We observed iron removal from chrysotile fibers in a dose-dependent manner (Fig. 5A). The control (succinate medium alone) showed only weak dissolution (0.034 $mg.L^{-1}$), whereas iron release was significantly higher in the presence of PVD from 0.30 $mg.L^{-1}$ at 25 µM to 0.96 $mg.L^{-1}$ at 150 µM. The amount of iron released by 200 µM PVD was similar to that released by 150 µM, showing that the PVD concentration was not a limiting factor. Indeed, 10% of the siderophore was in a PVD-Fe complex form at 200 µM. Thus, the reaction involved a proportion of apo-PVD which could be high enough to extract iron, indicating that the limiting factor could be the availability of iron. Mohanty et al. (2018) showed that iron removal from chrysotile fibers increased if the concentration of desferrioxamine was raised from 1 to 10 µM. Our results confirm this study and suggest that iron release is limited by iron availability. Siderophores are well known for their high affinity for iron and recently Schalk et al. (2011) demonstrated that other metals can also be chelated by the PVD of *P. aeruginosa*. However, no data are available on the capacity of PVD to complex magnesium. Given that the studied FAW contains chrysotile with an external brucite layer composed of magnesium, fiber alteration may result in magnesium solubilization. We thus evaluated the effect of $PVD_{mandelii}$ on magnesium dissolution as well as that of iron (Fig. 5B). We observed no effect on magnesium dissolution at any tested concentrations. A relatively high magnesium concentration was measured in the control (5.5 $mg.L^{-1}$), with no significative difference from the amount of magnesium dissolved by $PVD_{mandelii}$ (3.85 $mg.L^{-1}$ to 6.89 $mg.L^{-1}$), regardless of the concentration tested. pH is a well-known parameter that has been described to influence the dissolution of the chrysotile brucite layer (Choi and Smith, 1972; Gronow, 1987). An acidic environment could strongly favor magnesium ion leaching, whereas slower dissolution kinetics may occur at neutral pH. All

solutions in our study were adjusted to pH 7 and thus measured magnesium release may have been due to the pH.

4. Conclusions

We investigated the efficiency of various PVDs to scavenge iron from FAW and the ability of the best identified PVDs to degrade asbestos waste. Our results showed a significant iron extraction from FAW by all tested PVDs but with differences in efficiency according to the pyoverdines and the type of waste. PVD from *P. mandelii* extracted the higher amount of iron from chrysotile-gypsum, while PVD from *P. fluorescens* was the most efficient for amosite-gypsum. The kinetic profiles of iron extraction from chrysotile-gypsum by these pyoverdines highlighted a time-dependent dissolution. A long-term alteration of chrysotile-gypsum by $PVD_{aeruginosa}$ and $PVD_{mandelii}$ revealed an extraction limit after renewal cycles for a total of 42 days leading to a large decrease of iron content from chrysotile fibers structure. Moreover, $PVD_{mandelii}$ extracted iron from chrysotile-gypsum in concentration-dependent manner. Our research identified efficient pyoverdines in biodegradation of asbestos waste. The resulting PVD-Fe complex could be exploited as a valuable iron source. Further investigations might allow to consider the development of an eco-friendly asbestos treatment, using pyoverdines, in order to reduce asbestos-related environmental and health problems.

Acknowledgements

This work was supported by the French Environment and Energy Management Agency (ADEME), the French R&D plan for asbestos removal (PRDA) and SOMEZ (Mediterranean Company of Zeolites).

References

Albrecht-Gary, A.-M., Blanc, S., Rochel, N., Ocaktan, A.Z., Abdallah, M.A., 1994. Bacterial iron transport: Coordination properties of pyoverdin PaA, a peptidic siderophore of *Pseudomonas aeruginosa*. Inorg. Chem. 33, 6391–6402. https://doi.org/10.1021/ic00104a059

Aouad, G., Crovisier, J.-L., Damidot, D., Stille, P., Hutchens, E., Mutterer, J., Meyer, J.-M., Geoffroy, V.A., 2008. Interactions between municipal solid waste incinerator bottom ash and bacteria (*Pseudomonas aeruginosa*). Sci. Total Environ. 393, 385–393. https://doi.org/10.1016/j.scitotenv.2008.01.017

Balducci, G., Foresti, E., Lelli, M., Lesci, I.G., Marchetti, M., Pierini, F., Roveri, N., 2012. Process for treating an asbestos containing material. EP2428254A1.

Briskot, G., Taraz, K., Budzikiewicz, H., 1989. Bacterial constituents, XXXVII. pyoverdin-type siderophores from *Pseudomonas aeruginosa*. Liebigs Annalen der Chemie 1989, 375–384. https://doi.org/10.1002/jlac.198919890164

Budzikiewicz, H., Schröder, H., Taraz, K., 2014. Zur biogenese der *Pseudomonas*-siderophore: Der nachweis analoger strukturen eines pyoverdin-desferriferribactin-paares. Zeitschrift für Naturforschung C 47, 26–32. https://doi.org/10.1515/znc-1992-1-206

Chao, C.C., Aust, A.E., 1994. Effect of long-term removal of iron from asbestos by desferrioxamine B on subsequent mobilization by other chelators and induction of DNA single-strand breaks. Arch. Biochem. Biophys. 308, 64–69. https://doi.org/10.1006/abbi.1994.1009

Choi, I., Smith, R.W., 1972. Kinetic study of dissolution of asbestos fibers in water. J. Colloid Interface Sci. 40, 253–262. https://doi.org/10.1016/0021-9797(72)90014-8

Dabboussi, F., Hamze, M., Singer, E., Geoffroy, V., Meyer, J.-M., Izard, D., 2002. *Pseudomonas mosselii* sp. nov., a novel species isolated from clinical specimens. Int. J. Syst. Evol. Microbiol. 52, 363–376. https://doi.org/10.1099/00207713-52-2-363

Daghino, S., Martino, E., Perotto, S., 2010. Fungal weathering and implications in the solubilization of metals from soil and from asbestos fiber. Current research, technology and education topics in applied microbiology and microbial biotechnology 1, 329–338.

Daghino, S., Martino, E., Vurro, E., Tomatis, M., Girlanda, M., Fubini, B., Perotto, S., 2008. Bioweathering of chrysotile by fungi isolated in ophiolitic sites. FEMS Microbiol Lett 285, 242–249. https://doi.org/10.1111/j.1574-6968.2008.01239.x

David, S.R., Ihiawakrim, D., Regis, R., Geoffroy, V.A., 2019. Iron removal from raw asbestos by siderophores-producing *Pseudomonas*. J. Hazard. Mater. 121563. https://doi.org/10.1016/j.jhazmat.2019.121563

Douguet, D., Carteron, H., Janiaud, P., Pinhas, N., 1997. Effets sur la santé des principaux types d'exposition à l'amiante. Institut national de la santé et de la recherche médicale (INSERM).

Favero-Longo, S.E., Castelli, D., Fubini, B., Piervittori, R., 2009. Lichens on asbestos–cement roofs: Bioweathering and biocovering effects. J. Hazard. Mater. 162, 1300–1308. https://doi.org/10.1016/j.jhazmat.2008.06.060

Favero-Longo, S.E., Turci, F., Tomatis, M., Castelli, D., Bonfante, P., Hochella, M.F., Piervittori, R., Fubini, B., 2005. Chrysotile asbestos is progressively converted into a non-fibrous amorphous material by the chelating action of lichen metabolites. J. Environ. Monit. 7, 764–766. https://doi.org/10.1039/B507569F

389 Ferret, C., Sterckeman, T., Cornu, J.-Y., Gangloff, S., Schalk, I.J., Geoffroy, V.A., 2014.
390 Siderophore- promoted dissolution of smectite by fluorescent *Pseudomonas*. Environ.
391 Microbiol. Rep. 6, 459–467. https://doi.org/10.1111/1758-2229.12146

392 Gronow, J.R., 1987. The dissolution of asbestos fibres in water. Clay Minerals 22, 21–35.
393 https://doi.org/10.1180/claymin.1987.022.1.03

394 Hohlneicher, U., Hartmann, R., Taraz, K., Budzikiewicz, H., 2014. Pyoverdin, ferribactin,
395 azotobactin - a new triade of siderophores from *Pseudomonas chlororaphis* ATCC 9446 and its
396 relation to *Pseudomonas fluorescens* ATCC 13525. Zeitschrift für Naturforschung C 50, 337–
397 344. https://doi.org/10.1515/znc-1995-5-602

398 Jülich, M., Taraz, K., Budzikiewicz, H., Geoffroy, V., Meyer, J.-M., Gardan, L., 2014. The
399 structure of the pyoverdin isolated from various *Pseudomonas syringae* pathovars. Zeitschrift für
400 Naturforschung C 56, 687–694. https://doi.org/10.1515/znc-2001-9-1003

401 Meyer, J.M., Abdallah, M.A., 1978. The fluorescent pigment of *Pseudomonas fluorescens*:
402 Biosynthesis, purification and physicochemical properties. Microbiology 107, 319–328.
403 https://doi.org/10.1099/00221287-107-2-319

404 Meyer, J.-M., Gruffaz, C., Raharinosy, V., Bezverbnaya, I., Schäfer, M., Budzikiewicz, H., 2008.
405 Siderotyping of fluorescent *Pseudomonas*: Molecular mass determination by mass spectrometry
406 as a powerful pyoverdine siderotyping method. Biometals 21, 259–271.
407 https://doi.org/10.1007/s10534-007-9115-6

408 Meyer, J.-M., Stintzi, A., Coulanges, V., Shivaji, S., Voss, J.A., Taraz, K., Budzikiewic, H.,
409 1998. Siderotyping of fluorescent pseudomonads: Characterization of pyoverdines of
410 *Pseudomonas fluorescens* and *Pseudomonas putida* strains from Antarctica. Microbiology 144,
411 3119–3126. https://doi.org/10.1099/00221287-144-11-3119

412 Mohanty, S.K., Gonneau, C., Salamatipour, A., Pietrofesa, R.A., Casper, B., Christofidou-
413 Solomidou, M., Willenbring, J.K., 2018. Siderophore-mediated iron removal from chrysotile:
414 Implications for asbestos toxicity reduction and bioremediation. J. Hazard. Mater. 341, 290–296.
415 https://doi.org/10.1016/j.jhazmat.2017.07.033

416 Paolini, V., Tomassetti, L., Segreto, M., Borin, D., Liotta, F., Torre, M., Petracchini, F., 2019.
417 Asbestos treatment technologies. J. Mater. Cycles Waste Manag. 21, 205–226.
418 https://doi.org/10.1007/s10163-018-0793-7

419 Persmark, M., Frejd, T., Mattiasson, B., 1990. Purification, characterization, and structure of
420 pseudobactin 589 A, a siderophore from a plant growth promoting *Pseudomonas*. Biochemistry
421 29, 7348–7356. https://doi.org/10.1021/bi00483a026

422 Pollastri, S., D'Acapito, F., Trapananti, A., Colantoni, I., Andreozzi, G.B., Gualtieri, A.F., 2015.
423 The chemical environment of iron in mineral fibres. A combined X-ray absorption and
424 Mössbauer spectroscopic study. J. Hazard. Mater. 298, 282–293.
425 https://doi.org/10.1016/j.jhazmat.2015.05.010

426 Rajkumar, M., Vara Prasad, M.N., Freitas, H., Ae, N., 2009. Biotechnological applications of

427 serpentine soil bacteria for phytoremediation of trace metals. Crit. rev. biotechnol. 29, 120–130.
428 https://doi.org/10.1080/07388550902913772

429 Schalk, I.J., Hannauer, M., Braud, A., 2011. New roles for bacterial siderophores in metal
430 transport and tolerance. Environ. Microbiol. 13, 2844–2854. https://doi.org/10.1111/j.1462-
431 2920.2011.02556.x

432 Scherpereel, A., 2016. Amiante et pathologie respiratoire. La Presse Médicale, Médecine et
433 environnement 45, 117–132. https://doi.org/10.1016/j.lpm.2015.12.011

434 Spasiano, D., Luongo, V., Petrella, A., Alfè, M., Pirozzi, F., Fratino, U., Piccinni, A.F., 2017.
435 Preliminary study on the adoption of dark fermentation as pretreatment for a sustainable
436 hydrothermal denaturation of cement-asbestos composites. J. Clean. Prod. 166, 172–180.
437 https://doi.org/10.1016/j.jclepro.2017.08.029

438 Spasiano, D., Pirozzi, F., 2017. Treatments of asbestos containing wastes. J. Environ. Manage.
439 204, Part 1, 82–91. https://doi.org/10.1016/j.jenvman.2017.08.038

440 Teintze, M., Hossain, M.B., Barnes, C.L., Leong, J., Van der Helm, D., 1981. Structure of ferric
441 pseudobactin: A siderophore from a plant growth promoting *Pseudomonas*. Biochemistry 20,
442 6446–6457. https://doi.org/10.1021/bi00525a025

443 Toyokuni, S., 2009. Mechanisms of asbestos-induced carcinogenesis. Nagoya J. Med. Sci. 71, 1–
444 10.

445 Valko, M., Jomova, K., Rhodes, C.J., Kuča, K., Musílek, K., 2015. Redox- and non-redox-metal-
446 induced formation of free radicals and their role in human disease. Arch. Toxicol. 90, 1–37.
447 https://doi.org/10.1007/s00204-015-1579-5

448 Virta, R.L., 2002. Asbestos: Geology, mineralogy, mining, and uses. US Department of the
449 Interior. US Geological Survey.

450 Wang, D., Cullimore, D.R., 2010. Bacteriological challenges to asbestos cement water
451 distribution pipelines. J. Environ. Sci. 22, 1203–1208. https://doi.org/10.1016/S1001-
452 0742(09)60239-4

453 Wang, D., Cullimore, R., Hu, Y., Chowdhury, R., 2011. Biodeterioration of asbestos cement
454 (AC) pipe in drinking water distribution systems. Int. Biodeterior. Biodegrad. 65, 810–817.
455 https://doi.org/10.1016/j.ibiod.2011.05.004

456 Wasserbauer, R., Zadák, Z., Novotný, J., 1988. Nitrifying bacteria on the asbestos-cement roofs
457 of stable buildings. International Biodeterioration 24, 153–165. https://doi.org/10.1016/0265-
458 3036(88)90045-0

459 Wong-Lun-Sang, S., Bernardini, J.-J., Hennard, C., Kyslík, P., Dell, A., Abdallah, M.A., 1996.
460 Bacterial siderophores: Structure elucidation, 2D 1H and 13C NMR assignments of pyoverdins
461 produced by *Pseudomonas fluorescens* CHAO. Tetrahedron Lett. 37, 3329–3332.
462 https://doi.org/10.1016/0040-4039(96)00569-2

463

FIGURE LEGENDS:

Fig. 1. Concentration of iron dissolved from flocking asbestos waste, chrysotile-gypsum (A) and amosite-gypsum (B), in the presence of various pyoverdine-containing supernatants (SN) after 24 h of contact. Error bars indicate the standard errors of the means of three or five replicates. Bars with the same letter are not significantly different ($p > 0.05$, Kruskal-Wallis test, three or five replicates).

Fig. 2. Evolution of iron concentration extracted from chrysotile-gypsum waste over 24 h in the presence of *Pseudomonas aeruginosa* or *Pseudomonas mandelii* pyoverdine-containing supernatants (SN). Error bars indicate the standard errors of the means of five replicates.

Fig. 3. Iron removal from chrysotile-gypsum waste after renewal cycles of 24 or 96 h in the presence of 100 µM (T24-1 to T24-9 and T96-1 to T96-7) or 200 µM (T24-C and T96-C) *Pseudomonas aeruginosa* or *Pseudomonas mandelii* pyoverdine-containing supernatants (SN). Error bars indicate the standard errors of the means of five replicates.

Fig. 4. STEM images and STEM mapping of chrysotile-gypsum fibers after renewal cycles of 24 or 96 h in the presence of succinate medium (a and b) or *Pseudomonas mandelii* pyoverdine-containing supernatants (SN) (c and d). Large images obtained from the combination of the three distributions of Mg, Si, and Fe with analysis areas (a and c). Atomic ratios of Mg/Si and Fe/Si (b and d). (e) Comparison histogram after renewal cycles with succinate medium or *Pseudomonas mandelii* pyoverdine-containing supernatants.

Fig. 5. Effect of various concentrations of pyoverdine produced by *Pseudomonas mandelii* on iron (A) and magnesium (B) dissolution from chrysotile-gypsum waste after 48 h of contact. Error bars indicate the standard errors of the means of five replicates. Bars with the same letter are not significantly different ($p > 0.05$, Kruskal-Wallis test of five replicates).

Highlights

- Weathering efficiency varies according to the pyoverdines and the type of waste.
- Pyoverdines solubilize iron in a time-dependent manner.
- Chrysotile-gypsum weathering by pyoverdines decreases iron concentration in fibers.
- Iron removal from chrysotile-gypsum is concentration-dependent of pyoverdines.
- Pyoverdines could be used in bioremediation process of asbestos waste.

Table 1. List of pyoverdines used, with their molecular mass, isoelectrofocusing characteristics, and peptide composition.

Siderovars	Species	MM	Number of isoforms and pHi values		Pyoverdine peptide chain	References
Lille 1	*P. monteilii*	1 291	2	7.3/4.6	Asp–Lys–AcOHOrn–Ala–Ser–Ser–Gly–Ser–cOHOrn	Meyer et al. (2008)
Syr	*P. syringae*	1 123	2	5.0/4.0	εLys–OHAsp–Thr–(Thr–Ser–OHAsp–Ser)	Jülich et al. (2014)
B10/PL9/ 7SR1/A225	*P. lini*	989	3	7.5/5.2/4.6	εLys–OHAsp–Ala–aThr–Ala–cOHOrn	Teintze et al. (1981)
12633	*P. putida*	1 336	3	4.6/4.2/4.0	Asp–εLys–OHAsp–Ser–Thr–Ala–Glu–Ser cOHOrn	Persmark et al. (1990)
Lille 17	*P. mosselii*	-	3	9.0/7.4/5.2	ND	Dabboussi et al. (2002)
13525	*P. fluorescens*	1 160	3	8.7/7.3/7.1	Ser–Lys–Gly–FOHOrn–(Lys–FOHOrn–Ser)	Hohlneicher et al. (2014)
CHA0	*P. fluorescens*	1 287	3	8.5/7.5/5.1	Asp–FOHOrn–Lys–(Thr–Ala–Ala–FOHOrn–Lys)	Wong-Lun-Sang et al. (1996)
PAO1	*P. aeruginosa*	1 333	2	8.8/7.0	Ser–Arg–Ser–FOHOrn–(Lys–FOHOrn–Thr–Thr)	Briskot et al. (1989)
SB8.3	*P. mandelii*	1 046	3	9.0/8.8/7.6	Ala–Lys–Thr–Ser–AOHOrn–cOHOrn	Budzikiewicz et al. (2014)

εLys: lys linked by its ε-NH2; OHAsp: threo-β-hydroxy-aspartic acid; aThr: allo-Thr; cOHOrn: cyclo-hydroxy-ornithine; FOHOrn: δN -formyl- δN -hydroxy-ornithine; AOHOrn δN -acetyl- δN -hydroxy-ornithine.

Parentheses indicate cyclic structures. D-amino acids are underlined. A broken line means that the two enantiomers were detected among the underlined residues. ND: not determined.

Figure

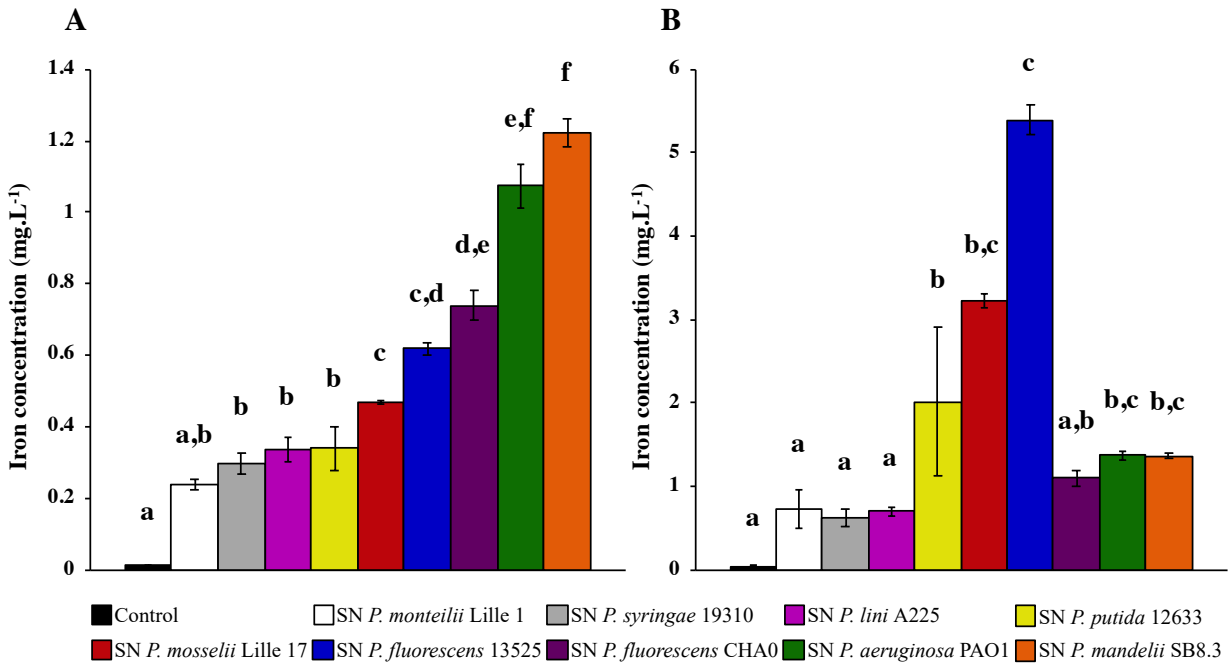

Fig. 1. Concentration of iron dissolved from flocking asbestos waste, chrysotile-gypsum (A) and amosite-gypsum (B), in the presence of various pyoverdine-containing supernatants (SN) after 24 h of contact. Error bars indicate the standard errors of the means of three or five replicates. Bars with the same letter are not significantly different ($p > 0.05$, Kruskal-Wallis test, three or five replicates).

In color online

Figure

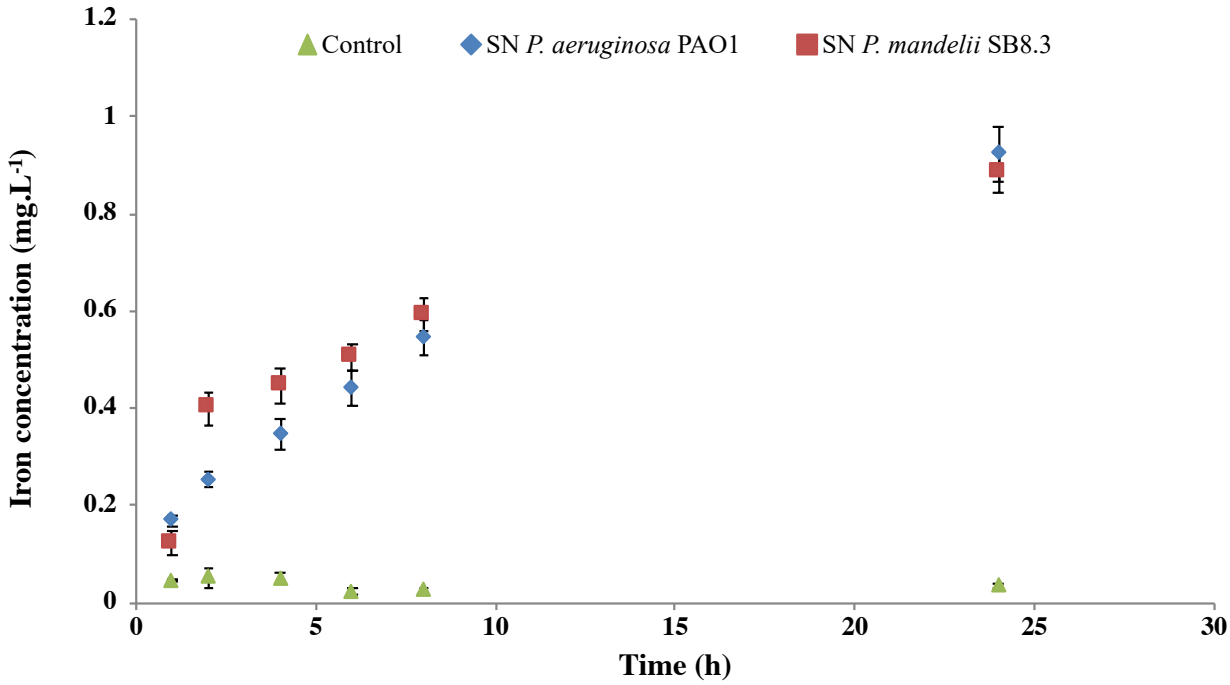

Fig. 2. Evolution of iron concentration extracted from chrysotile-gypsum waste over 24 h in the presence of *Pseudomonas aeruginosa* or *Pseudomonas mandelii* pyoverdine-containing supernatants (SN). Error bars indicate the standard errors of the means of five replicates.

In color online

Figure

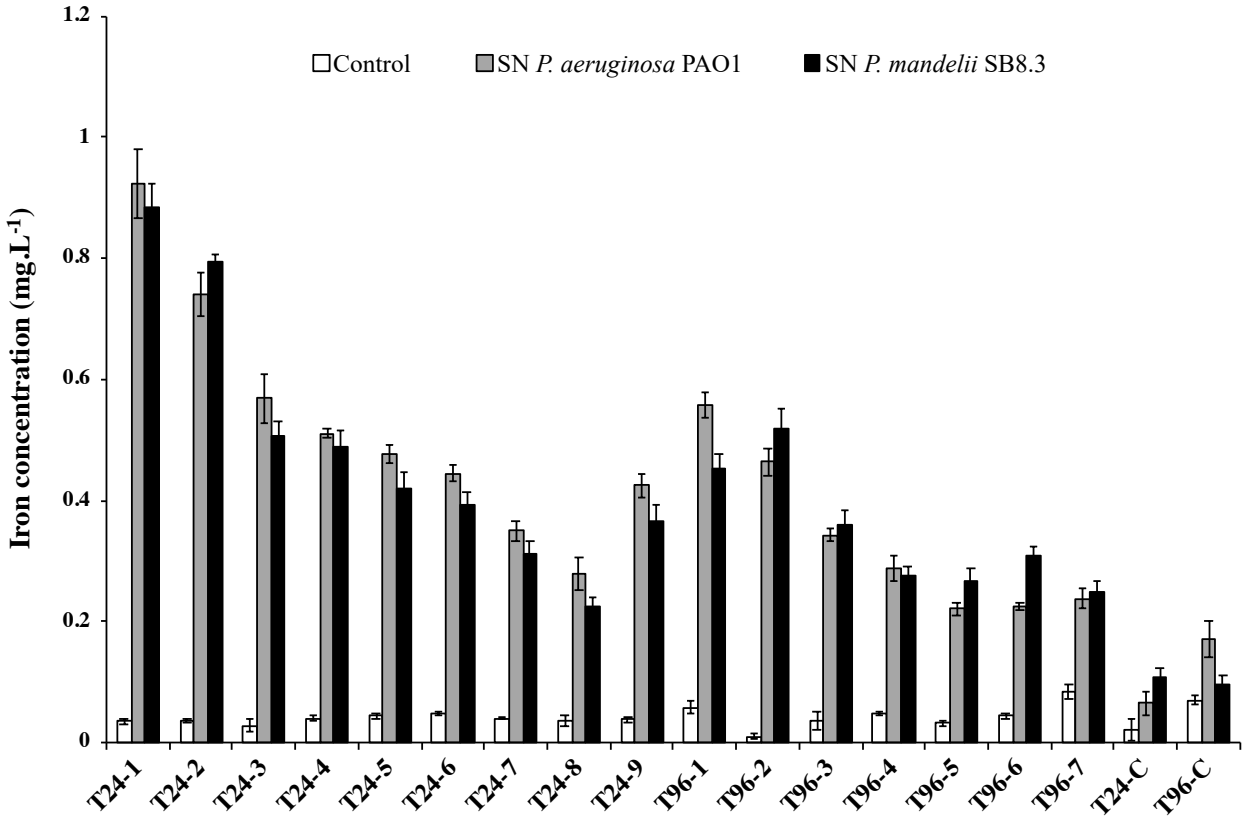

Fig. 3. Iron removal from chrysotile-gypsum waste after renewal cycles of 24 or 96 h in the presence of 100 µM (T24-1 to T24-9 and T96-1 to T96-7) or 200 µM (T24-C and T96-C) *Pseudomonas aeruginosa* or *Pseudomonas mandelii* pyoverdine-containing supernatants (SN). Error bars indicate the standard errors of the means of five replicates.

Figure

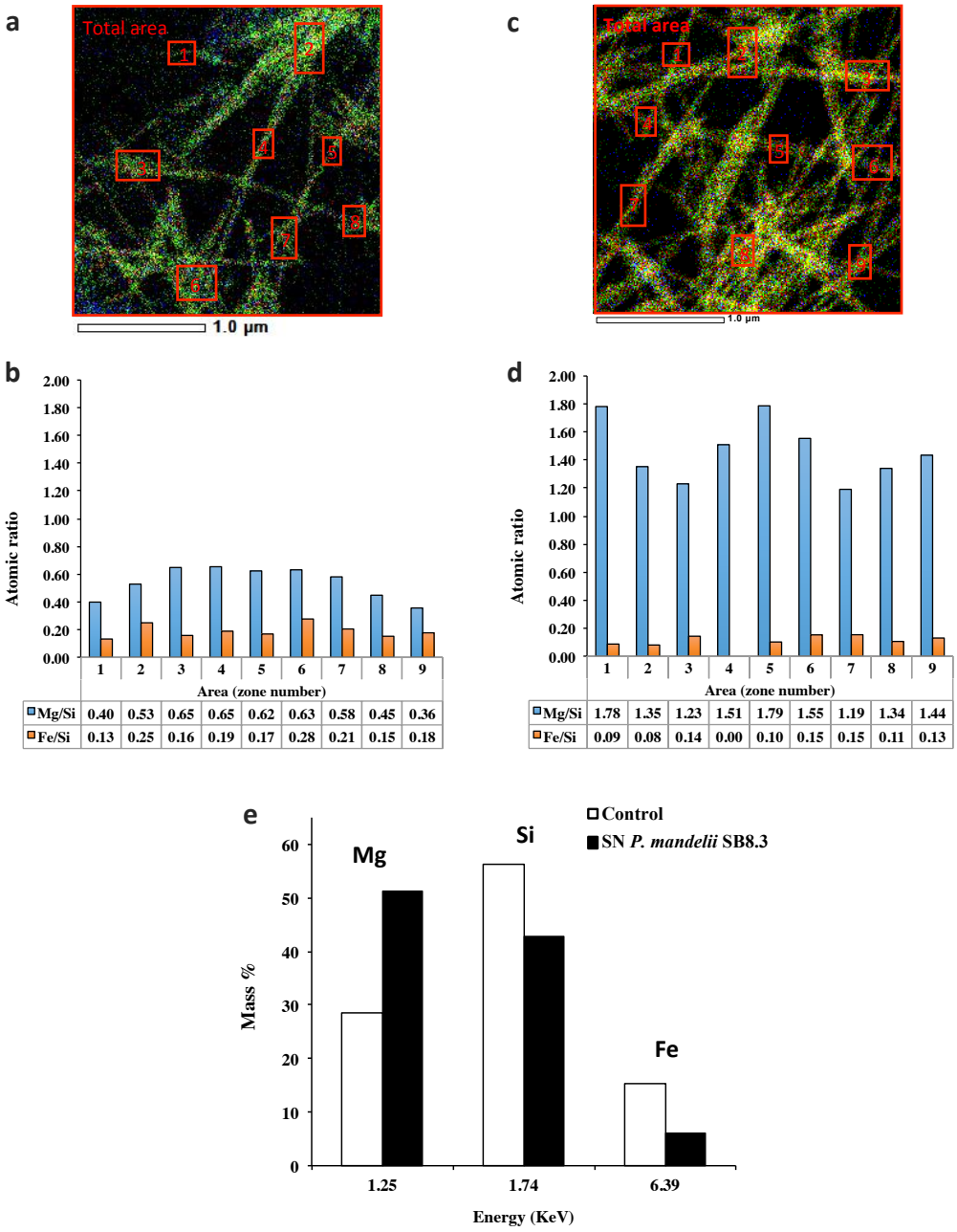

Fig. 4. STEM images and STEM mapping of chrysotile-gypsum fibers after renewal cycles of 24 or 96 h in the presence of succinate medium (a and b) or *Pseudomonas mandelii* pyoverdine-containing supernatants (SN) (c and d). Large images obtained from the combination of the three distributions of Mg, Si, and Fe with analysis areas (a and c). Atomic ratios of Mg/Si and Fe/Si (b and d). (e) Comparison histogram after renewal cycles with succinate medium or *Pseudomonas mandelii* pyoverdine-containing supernatants.

In color online

Figure

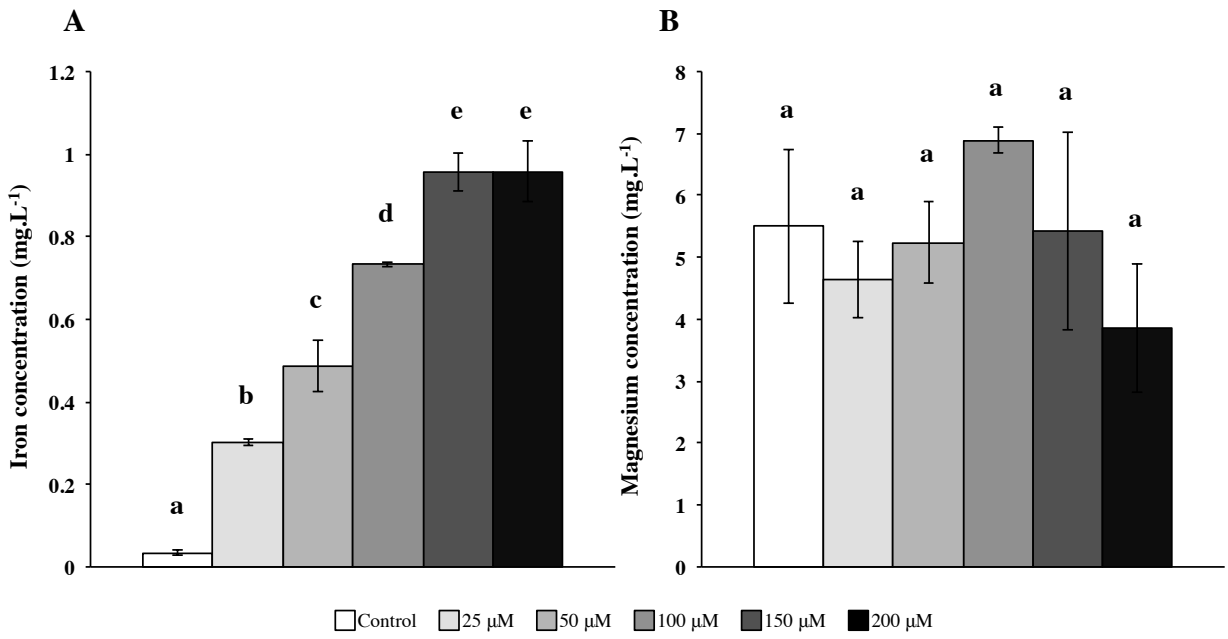

Fig. 5. Effect of various concentrations of pyoverdine produced by *Pseudomonas mandelii* on iron (A) and magnesium (B) dissolution from chrysotile-gypsum waste after 48 h of contact. Error bars indicate the standard errors of the means of five replicates. Bars with the same letter are not significantly different ($p > 0.05$, Kruskal-Wallis test of five replicates).

1 **Graphical Abstract**

2

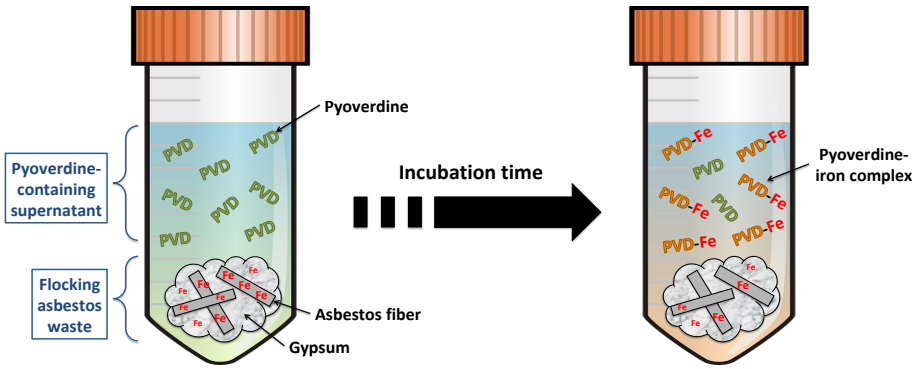

3

4